

Nonreciprocal coupling induced entanglement enhancement in a double-cavity optomechanical system

Yuan-Yuan Liu(刘元元), Zhi-Ming Zhang(张智明), Jun-Hao Liu(刘军浩), Jin-Dong Wang(王金东), and Ya-Fei Yu(於亚飞)

Citation: Chin. Phys. B, 2022, 31 (**9**): 094203. DOI: 10.1088/1674-1056/ac6499
Journal homepage: http://cpb.iphy.ac.cn; http://iopscience.iop.org/cpb

What follows is a list of articles you may be interested in

Bright 547-dimensional Hilbert-space entangled resource in 28-pair modes biphoton frequency comb from a reconfigurable silicon microring resonator

Qilin Zheng(郑骑林), Jiacheng Liu(刘嘉成), Chao Wu(吴超), Shichuan Xue(薛诗川), Pingyu Zhu(朱枰谕), Yang Wang(王洋), Xinyao Yu(于馨瑶), Miaomiao Yu(余苗苗), Mingtang Deng(邓明堂), Junjie Wu(吴俊杰), and Ping Xu(徐平)

Chin. Phys. B, 2022, 31 (**2**): 024206. DOI: 10.1088/1674-1056/ac3507

Quantum speed limit time and entanglement in a non-Markovian evolution of spin qubits of coupled quantum dots

M. Bagheri Harouni

Chin. Phys. B, 2020, 29 (**12**): 124203. DOI: 10.1088/1674-1056/abab75

Reversion of weak-measured quantum entanglement state

Shao-Jiang Du(杜少将), Yonggang Peng(彭勇刚), Hai-Ran Feng(冯海冉), Feng Han(韩峰), Lian-Wu Yang(杨连武), Yu-Jun Zheng(郑雨军)

Chin. Phys. B, 2020, 29 (**7**): 074202. DOI: 10.1088/1674-1056/ab8c3e

Entangling two oscillating mirrors in an optomechanical system via a flying atom

Yu-Bao Zhang(张玉宝), Jun-Hao Liu(刘军浩), Ya-Fei Yu(於亚飞), Zhi-Ming Zhang(张智明)

Chin. Phys. B, 2018, 27 (**7**): 074209. DOI: 10.1088/1674-1056/27/7/074209

Generation of entangled TEM_{01} modes withperiodically poled $KTiOPO_4$ crystal

Rong-Guo Yang(杨荣国), Jing-jing Wang(王晶静), Jing Zhang(张静), Heng-Xin Sun(孙恒信)

Chin. Phys. B, 2016, 25 (**7**): 074208. DOI: 10.1088/1674-1056/25/7/074208

Nonreciprocal coupling induced entanglement enhancement in a double-cavity optomechanical system

Yuan-Yuan Liu(刘元元)[1], Zhi-Ming Zhang(张智明)[2], Jun-Hao Liu(刘军浩)[1,†], Jin-Dong Wang(王金东)[2,‡], and Ya-Fei Yu(於亚飞)[1,§]

[1] *Guangdong Provincial Key Laboratory of Nanophotonic Functional Materials and Devices (School of Information and Optoelectronic Science and Engineering), South China Normal University, Guangzhou* 510006, *China*

[2] *Guangdong Provincial Key Laboratory of Quantum Engineering and Quantum Materials, South China Normal University, Guangzhou* 510006, *China*

(Received 23 January 2022; revised manuscript received 16 March 2022; accepted manuscript online 6 April 2022)

We investigate the quantum entanglement in a double-cavity optomechanical system consisting of an optomechanical cavity and an auxiliary cavity, where the optomechanical cavity mode couples with the mechanical mode via radiation-pressure interaction, and simultaneously couples with the auxiliary cavity mode via nonreciprocal coupling. We study the entanglement between the mechanical oscillator and the cavity modes when the two cavities are reciprocally or nonreciprocally coupled. The logarithmic negativity $E_n^{(1)}$ ($E_n^{(2)}$) is adopted to describe the entanglement degree between the mechanical mode and the optomechanical cavity mode (the auxiliary cavity mode). We find that both $E_n^{(1)}$ and $E_n^{(2)}$ have maximum values in the case of reciprocal coupling. By using nonreciprocal coupling, $E_n^{(1)}$ and $E_n^{(2)}$ can exceed those maximum values, and a wider detuning region where the entanglement exists can be obtained. Moreover, the entanglement robustness with respect to the environment temperature is also effectively enhanced.

Keywords: quantum entanglement, double-cavity optomechanical system, nonreciprocal coupling

PACS: 42.50.–p, 42.50.Pq, 42.82.Fv **DOI:** 10.1088/1674-1056/ac6499

1. Introduction

Cavity optomechanics[1,2] is the study of the radiation pressure interaction between the optical cavity field and the mechanical motion. In general, a cavity optomechanical system (COMS) consists of a Fabry–Perot cavity with one movable mirror, where the cavity mode couples with the mechanical mode via radiation pressure. COMS has attracted increasing attention due to its prominent applications in gravitational-wave detection,[3] photonic network,[4] metrology,[5] etc. With the rapid development of nanotechnology, COMS also provides a substantial platform for exploring quantum effects in an exceedingly wide range from microscale to macroscale, for instance, entanglement,[6–9] squeezing,[10–13] photon blockade,[14–18] transmission,[19] etc. As is known, entanglement is an enigmatic phenomenon in quantum mechanics and its detailed study would be beneficial. Firstly, it can help us identify the boundary between the classical and quantum worlds.[20] Secondly, it has numerous potential applications in quantum technology and science, such as quantum computation,[21] quantum communication,[22] quantum metrology,[23] etc.

In recent years, great efforts have been made to explore quantum entanglement in various hybrid COMSs. In 2007, Vitali *et al.* investigated the steady-state entanglement between the cavity mode and the movable mirror in a standard COMS.[24] In 2012, three photomechanical cavity arrays coupled reversibly or irreversibly to each other were studied, and it was found that this composite system exhibits photon–phonon entanglement between cavities.[25] Then, Liao *et al.* proposed a scheme to generate quantum entanglement between two mechanical resonators in a two-cavity optomechanical system in 2014.[26] Later, Liu *et al.* proposed a scheme to generate the entanglement between two COMS via a flying two-level atom in 2017,[27] and Xu *et al.* explored a scheme to generate single entangled photon–phonon pair in a hybrid COMS via atom-photon–phonon interaction in 2019.[28] Recently, Jiao *et al.* showed how to achieve the nonreciprocal entanglement in a COMS.[29]

At present, the non-Hermitian systems have drawn extensive interest because of its novel properties.[30,31] There are two kinds of implementation schemes, i.e., the gain systems[32,33] and the nonreciprocally coupled systems.[34–36] Here, the objective is to study the quantum entanglement in a nonreciprocally coupled system. Therefore, we propose a double-cavity optomechanical system, which is composed of an optomechanical cavity and an auxiliary cavity. In this system, the optomechanical cavity mode couples with the mechanical mode via radiation-pressure interaction, and couples with the auxiliary cavity mode via nonreciprocal coupling.[37] Such a kind of nonreciprocal coupling can be achieved by us-

†Corresponding author. E-mail: jhliu@m.scnu.edu.cn
‡Corresponding author. E-mail: wangjindong@m.scnu.edu.cn
§Corresponding author. E-mail: yuyafei@m.scnu.edu.cn

© 2022 Chinese Physical Society and IOP Publishing Ltd

ing an imaginary gauge field,[38,39] impurity,[40] or auxiliary nonreciprocal transition device.[41,42] We adopt the logarithmic negativity $E_n^{(1)}$ ($E_n^{(2)}$) to quantify the entanglement degree between the mechanical mode and the optomechanical cavity mode (the auxiliary cavity mode). We find that both $E_n^{(1)}$ and $E_n^{(2)}$ have maximum values in the case of reciprocal coupling. By using the nonreciprocal coupling, $E_n^{(1)}$ and $E_n^{(2)}$ can exceed those maximum values, and a wider detuning region where the entanglement exists can be obtained. Moreover, the entanglement robustness with respect to the environment temperature can be effectively enhanced.

This paper is organized as follows. In Section 2, we present the Hamiltonian of the system and derive the Heisenberg–Langevin equations. Furthermore, we introduce the logarithmic negativity to quantify the entanglement degree between the mechanical mode and the optical cavity modes. In Section 3, we demonstrate the nonreciprocal coupling induced enhancement of the entanglement degree and entanglement robustness. Finally, a brief summary is given in Section 4.

2. Model and analytical expressions

As shown in Fig. 1, we consider a cavity optomechanical system where the cavity mode ($\hat{a}_1$) couples with the mechanical mode ($\hat{p}$, $\hat{q}$) via radiation pressure, and an auxiliary cavity mode ($\hat{a}_2$) couples with the optomechanical cavity mode ($\hat{a}_1$) via nonreciprocal interaction. In a frame rotating at the frequency ω_l of the driving field, the total Hamiltonian of the non-Hermitian system can be expressed as follows:

$$\begin{aligned} H/\hbar =& \sum_{j=1}^{2}\Delta_j\hat{a}_j^\dagger\hat{a}_j+\frac{\omega_{\rm m}}{2}(\hat{p}^2+\hat{q}^2)-G_0\hat{a}_1^\dagger\hat{a}_1\hat{q}\\ &+J_1\hat{a}_1^\dagger\hat{a}_2+J_2\hat{a}_2^\dagger\hat{a}_1+{\rm i}\varepsilon_l(\hat{a}_2^\dagger-\hat{a}_2), \end{aligned} \tag{1}$$

where the first term is the free Hamiltonian of the cavity modes with the annihilation and creation operators $\hat{a}_j$ and $\hat{a}_j^\dagger$, and $\Delta_j=\omega_j-\omega_l$ is the corresponding cavity–laser detuning. The second term denotes the Hamiltonian of the mechanical oscillator with $\hat{q}$ and $\hat{p}$ being the position and momentum operators, respectively. The third term describes the optomechanical interaction, where $G_0=x_{\rm zpf}\omega_1/L$ is the single-photon optomechanical coupling strength ($x_{\rm zpf}=\sqrt{\hbar/2m\omega_{\rm m}}$ is the zero-point fluctuation, m is the effective mass of the mechanical mode, and L is the length of the optomechanical cavity). The fourth and fifth terms describe the nonreciprocal coupling between the optomechanical cavity mode ($\hat{a}_1$) and the auxiliary cavity mode ($\hat{a}_2$), and J_1 (J_2) represents the tunneling strength of photon jumping into cavity $\hat{a}_1$ ($\hat{a}_2$). The last term is the interaction Hamiltonian between the auxiliary cavity mode and the outer driving field. The amplitude of the driving field is $\varepsilon_l=\sqrt{2\kappa_2 P/\hbar\omega_l}$, where κ_2 denotes the decay rate of the auxiliary cavity and P refers to the input power.

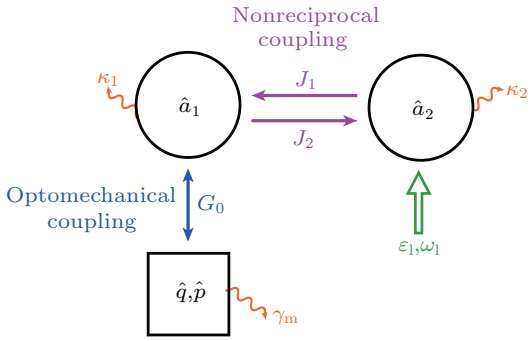


Fig. 1. Schematic diagram of the double cavity optomechanical system with nonreciprocal coupling. G_0 denotes the single photon optomechanical coupling strength, J_1 (J_2) represents the tunneling strength of photon jumping into cavity $\hat{a}_1$ ($\hat{a}_2$). ε_l (ω_l) is the amplitude (frequency) of the pump field. κ_1 (κ_2) is the decay rate of the cavity mode $\hat{a}_1$ ($\hat{a}_2$), and $\gamma_{\rm m}$ is the mechanical damping rate.

By using the Hamiltonian and introducing the dissipation and fluctuation terms, the Heisenberg–Langevin equations can be written as

$$\begin{aligned} \dot{\hat{a}}_1 &= -({\rm i}\Delta_1+\kappa_1)\hat{a}_1-{\rm i}J_1\hat{a}_2+{\rm i}G_0\hat{a}_1\hat{q}+\sqrt{2\kappa_1}\hat{a}_{1,{\rm in}},\\ \dot{\hat{a}}_2 &= -({\rm i}\Delta_2+\kappa_2)\hat{a}_2-{\rm i}J_2\hat{a}_1+\varepsilon_l+\sqrt{2\kappa_2}\hat{a}_{2,{\rm in}},\\ \dot{\hat{q}} &= \omega_{\rm m}\hat{p},\\ \dot{\hat{p}} &= -\omega_{\rm m}\hat{q}-\gamma_{\rm m}\hat{p}+G_0\hat{a}_1^\dagger\hat{a}_1+\hat{\xi}, \end{aligned} \tag{2}$$

where κ_1 is the decay rate of the optomechanical cavity, $\gamma_{\rm m}$ is the mechanical damping rate, $\hat{a}_{j,{\rm in}}$ and $\hat{\xi}$ are the fluctuation operators corresponding to the cavity modes and the mechanical mode, respectively, and obey the following correlation functions:[43]

$$\begin{aligned} \langle\hat{a}_{j,{\rm in}}(t)\hat{a}_{j,{\rm in}}^\dagger(t')\rangle &= \delta(t-t'),\\ \langle\hat{\xi}(t)\hat{\xi}(t')\rangle &= \gamma_{\rm m}(2n_{\rm m}+1)\delta(t-t'), \end{aligned} \tag{3}$$

while $n_{\rm m}=[\exp(\hbar\omega_{\rm m}/k_{\rm B}T)-1]^{-1}$ denotes the thermal photon number, $k_{\rm B}$ is the Boltzmann constant and T is the temperature of the mechanical oscillator. Their mean values $\langle\hat{a}_{j,{\rm in}}(t)\rangle=\langle\hat{\xi}(t)\rangle=0$.

Under the condition of strong optical driving, the nonlinear Eq. (2) can be linearized by rewriting each operator as a sum of its steady-state mean value plus a small fluctuation around it, i.e.,

$$\hat{a}_j=\alpha_j+\delta\hat{a}_j,\quad \hat{q}=q_s+\delta\hat{q},\quad \hat{p}=p_s+\delta\hat{p}. \tag{4}$$

By substituting the above ansatz Eq. (4) into Eq. (2), the equations will be decoupled into a set of nonlinear algebraic equations for the steady-state mean values and a set of quantum Heisenberg–Langevin equations for the fluctuation operators. The steady-state mean values can be obtained by setting the time derivatives to zero, as follows:

$$\begin{aligned} \alpha_1 &= \frac{-{\rm i}J_1\alpha_2}{{\rm i}\Delta_1'+\kappa_1},\quad \alpha_2=\frac{\varepsilon_l-{\rm i}J_2\alpha_1}{{\rm i}\Delta_2+\kappa_2},\\ q_s &= \frac{G_0|\alpha_1|^2}{\omega_{\rm m}},\quad p_s=0, \end{aligned} \tag{5}$$

where $\Delta_1' = \Delta_1 - G_0 q_s$ is the effective detuning. The quantum Heisenberg–Langevin equations for the fluctuation operators can be expressed as follows:

$$\begin{aligned}
\delta\dot{\hat{X}}_1 &= \Delta_1'\delta\hat{Y}_1 - \kappa_1\delta\hat{X}_1 + J_1\delta\hat{Y}_2 - G_y\delta\hat{q} + \sqrt{2\kappa_1}\hat{X}_{1,\mathrm{in}},\\
\delta\dot{\hat{Y}}_1 &= -\Delta_1'\delta\hat{X}_1 - \kappa_1\delta\hat{Y}_1 - J_1\delta\hat{X}_2 + G_x\delta\hat{q} + \sqrt{2\kappa_1}\hat{Y}_{1,\mathrm{in}},\\
\delta\dot{\hat{X}}_2 &= \Delta_2\delta\hat{Y}_2 - \kappa_2\delta\hat{X}_2 + J_1\delta\hat{Y}_1 + \sqrt{2\kappa_2}\hat{X}_{2,\mathrm{in}},\\
\delta\dot{\hat{Y}}_2 &= -\Delta_2\delta\hat{X}_2 - \kappa_2\delta\hat{Y}_2 - J_1\delta\hat{X}_1\sqrt{2\kappa_2}\hat{Y}_{2,\mathrm{in}},\\
\delta\dot{\hat{q}} &= \omega_{\mathrm{m}}\delta\hat{p},\\
\delta\dot{\hat{p}} &= -\omega_{\mathrm{m}}\delta\hat{q} - \gamma_{\mathrm{m}}\delta\hat{p} + G_0(\alpha_1^*\delta\hat{a}_1 + \delta\hat{a}_1^\dagger\alpha_1) + \hat{\xi},
\end{aligned} \tag{6}$$

Here, we have defined the operators of the quadrature fluctuations and the corresponding input noises as

$$\begin{aligned}
\delta\hat{X}_j &= \frac{1}{\sqrt{2}}(\delta\hat{a}_j^\dagger + \delta\hat{a}_j), \quad \delta\hat{Y}_j = \frac{\mathrm{i}}{\sqrt{2}}(\delta\hat{a}_j^\dagger - \delta\hat{a}_j),\\
\hat{X}_{j,\mathrm{in}} &= \frac{1}{\sqrt{2}}(\hat{a}_{j,\mathrm{in}}^\dagger + \hat{a}_{j,\mathrm{in}}), \quad \hat{Y}_{j,\mathrm{in}} = \frac{\mathrm{i}}{\sqrt{2}}(\hat{a}_{j,\mathrm{in}}^\dagger - \hat{a}_{j,\mathrm{in}}),
\end{aligned} \tag{7}$$

and G_x (G_y) is the real (imaginary) part of the effective optomechanical coupling strength $G = \sqrt{2}G_0\alpha_1$. Then, Eq. (6) can be rewritten compactly by introducing the vectors $u^{\mathrm{T}}(t) = (\delta\hat{X}_1, \delta\hat{Y}_1, \delta\hat{X}_2, \delta\hat{Y}_2, \delta\hat{q}, \delta\hat{p})$, and $v^{\mathrm{T}}(t) = (\sqrt{2\kappa_1}\hat{X}_{1,\mathrm{in}}, \sqrt{2\kappa_1}\hat{Y}_{1,\mathrm{in}}, \sqrt{2\kappa_2}\hat{X}_{2,\mathrm{in}}, \sqrt{2\kappa_2}\hat{Y}_{2,\mathrm{in}}, 0, \hat{\xi})$, i.e.,

$$\dot{u}(t) = Au(t) + v(t), \tag{8}$$

where $u(t) = M(t)u(0) + \int_0^t \mathrm{d}\tau M(\tau)v(t-\tau)$, $M(t) = \exp(At)$, and the matrix A describes the response of the system and is explicitly given by

$$A = \begin{pmatrix}
-\kappa_1 & \Delta_1' & 0 & J_1 & -G_y & 0\\
-\Delta_1' & -\kappa_1 & -J_1 & 0 & G_x & 0\\
0 & J_2 & -\kappa_2 & \Delta_2 & 0 & 0\\
-J_2 & 0 & -\Delta_2 & -\kappa_2 & 0 & 0\\
0 & 0 & 0 & 0 & 0 & \omega_{\mathrm{m}}\\
G_x & G_y & 0 & 0 & -\omega_{\mathrm{m}} & -\gamma_{\mathrm{m}}
\end{pmatrix}. \tag{9}$$

The system is stable when all real parts of the eigenvalues of A are negative. The stability conditions can be obtained by using the Routh–Hurwitz criterion.[44] Under the stability conditions, we have $M(\infty) = 0$ and

$$u_i(\infty) = \int_0^\infty \mathrm{d}\tau \sum_k M_{ik}(\tau)v_k(t-\tau). \tag{10}$$

Due to the Gaussian properties of the quantum noises and the linearized dynamics, the quantum steady state for the fluctuations is a tripartite zero-mean Gaussian state, which can be fully characterized by its 6×6 correlation matrix V, with its component

$$V_{kl} = \langle u_k(\infty)u_l(\infty) + u_l(\infty)u_k(\infty)\rangle/2\,. \tag{11}$$

By plugging Eq. (10) into Eq. (11), we get the following equation:

$$V = \int_0^\infty \mathrm{d}\tau M(\tau)DM^{\mathrm{T}}(\tau), \tag{12}$$

in which

$$D = \mathrm{Diag}[\kappa_1, \kappa_1, \kappa_2, \kappa_2, 0, \gamma_{\mathrm{m}}(2\mathrm{n}_{\mathrm{m}} + 1)] \tag{13}$$

is the diagonal matrix and defined by

$$\langle v_k(\tau)v_l(\tau') + v_l(\tau')v_k(\tau)\rangle/2 = D_{kl}\delta(\tau - \tau').$$

When the system is stable, the steady-state correlation matrix V fulfills the Lyapunov equation

$$AV + VA^{\mathrm{T}} = -D. \tag{14}$$

In this paper, we use the logarithmic negativity to measure the entanglement between the mechanical mode and the optical mode,[45] and

$$E_n = \max[0, -\ln 2\mathcal{V}], \tag{15}$$

where $\mathcal{V} = 2^{-1/2}\{\sum(V') - [\sum(V')^2 - 4\det V']^{1/2}\}^{1/2}$, and $\sum V' = \det\mathcal{A} + \det\mathcal{B} - 2\det\mathcal{C}$. By tracing out one mode in V and writing it in a 2×2 block form

$$V' = \begin{pmatrix} \mathcal{A} & \mathcal{C} \\ \mathcal{C}^{\mathrm{T}} & \mathcal{B} \end{pmatrix}, \tag{16}$$

the entanglement will emerge in the corresponding subsystem if and only if $\mathcal{V} < 1/2$.

In the following numerical simulations, to ensure the stability of the system, we use the experimentally feasible parameters[46–48] $L = 1$ mm, $\lambda_l = 810$ nm, $P = 35$ mW, and $\omega_{\mathrm{m}}/2\pi = 10$ MHz. We also assume that the two cavities have the same decay rate, i.e., $\kappa_1/2\pi = \kappa_2/2\pi = \kappa/2\pi = 5$ MHz, and $m = 5$ ng, $\gamma_{\mathrm{m}}/2\pi = 100$ Hz. Moreover, we assume that $\Delta_2 = -\Delta_1' = \Delta$.[49]

3. Numerical simulations

3.1. Nonreciprocal coupling induced entanglement enhancement

In this section, we study the entanglement degree between the mechanical oscillator and the cavity modes when the two cavities are reciprocally or nonreciprocally coupled. The logarithmic negativity $E_n^{(1)}$ ($E_n^{(2)}$) describes the entanglement degree between the mechanical mode and the optomechanical cavity mode (the auxiliary cavity mode).

Figure 2 shows $E_n^{(1)}$ and $E_n^{(2)}$ in the case of reciprocal coupling, i.e., $J_1 = J_2 = J$. As shown in Fig. 2(a), $E_n^{(1)}$ is plotted as a function of the detuning Δ with different values of J. It can be seen that, with the increase in value of Δ, $E_n^{(1)}$ firstly remains at zero, then increases to a peak value, and finally decreases to zero again. Besides, the peak value increases and then decreases with increasing J. For example, if $J = 0.4\kappa$ (blue solid line), $E_n^{(1)}$ is equal to zero when $\Delta < 0.15\omega_{\mathrm{m}}$, then increases to the peak value 0.15 when $\Delta = 0.35\omega_{\mathrm{m}}$, and finally decreases to zero when $\Delta = 1.1\omega_{\mathrm{m}}$. Specifically, $E_n^{(1)}$ reaches its maximum value 0.25 when $J = 0.8\kappa$ and $\Delta = 0.4\omega_{\mathrm{m}}$. To

see a wider parameter space, $E_n^{(1)}$ is plotted as functions of Δ and J in Fig. 2(b). We can intuitively see that there exists a maximum value of $E_n^{(1)}$. In Fig. 2(c), $E_n^{(2)}$ is plotted as a function of the detuning Δ with different values of J, and we find that $E_n^{(2)}$ has the similar variation tendency as that of $E_n^{(1)}$. When $J = 2\kappa$ and $\Delta = 0.6\omega_{\rm m}$, $E_n^{(2)}$ has the maximum value 0.27, which can be also clearly seen in Fig. 2(d).

Figure 3 displays, the logarithmic negativity $E_n^{(1)}$ and $E_n^{(2)}$ in the case of nonreciprocal coupling, i.e., $J_1 \neq J_2$. As shown in Fig. 3(a), $E_n^{(1)}$ is plotted as a function of the detuning Δ with different values of J_2, and we have assumed that $J_1 = 0.8\kappa$. When $J_2 = 0.8\kappa$ (the blue solid line), this system is reduced to the case of reciprocal coupling, and the maximum value of $E_n^{(1)}$ is 0.25. However, we find that $E_n^{(1)}$ can exceed that maximum value when $J_2 > 0.8\kappa$, and continues to increase with the increase in value of J_2. For instance, $E_n^{(1)}$ can reach 0.4 when $J_2 = 5\kappa$. Moreover, we can see that the detuning range where the entanglement exists is much larger than that in Fig. 2(a). The above results can be also explicitly seen in Fig. 3(b). In Fig. 3(c), $E_n^{(2)}$ is plotted as a function of the detuning Δ with different values of J_1, and $J_2 = 2\kappa$. Similarly, $E_n^{(2)}$ can exceed the maximum value 0.27 in the case of reciprocal coupling, and continues to increase with the increase in value of J_1. When $J_1 = 6\kappa$, the maximum value of $E_n^{(2)}$ can increase to 0.39. The detuning range where the entanglement exists is also much larger than that in Fig. 2(c). The intuitive results can be seen in Fig. 3(d) as well.

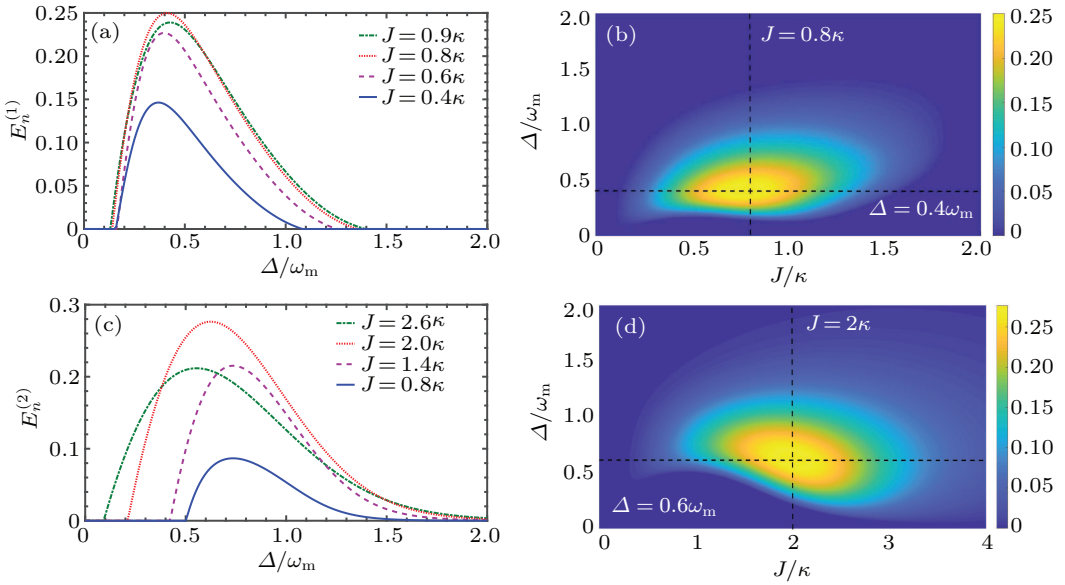


Fig. 2. (a), (c) The logarithmic negativity $E_n^{(1)}$ and $E_n^{(2)}$ as a function of the detuning Δ with different values of reciprocal coupling strength J. (b), (d) $E_n^{(1)}$ and $E_n^{(2)}$ as functions of Δ and J. The detailed parameters can be found in the text.

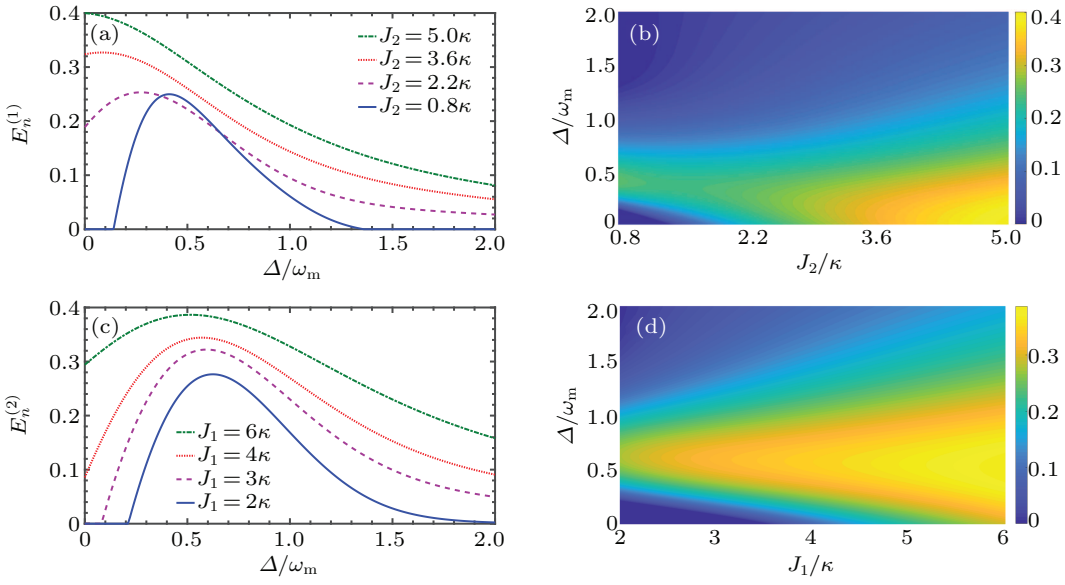


Fig. 3. (a) The logarithmic negativity $E_n^{(1)}$ as a function of the detuning Δ with different values of nonreciprocal coupling strength J_2. (b) $E_n^{(1)}$ as functions of Δ and J_2. (c) The logarithmic negativity $E_n^{(2)}$ as a function of the detuning Δ with different values of nonreciprocal coupling strength J_1. (d) $E_n^{(2)}$ as functions of Δ and J_1. (a), (b) $J_1 = 0.8\kappa$, (c), (d) $J_2 = 2\kappa$, and the other parameters are shown in the text.

3.2. Nonreciprocal coupling induced robustness enhancement

In this section, we show that the nonreciprocal coupling results in an enhancement of the entanglement robustness with respect to the environment temperature. Using similar methodology, we compare the influence of environment temperature T on the logarithmic negativity $E_n^{(1)}$ and $E_n^{(2)}$ in the case of reciprocal and nonreciprocal coupling.

As shown in Fig. 4(a), the logarithmic negativity $E_n^{(1)}$ is plotted as a function of the environment temperature T with different values of reciprocal coupling strength J. It can be seen that $E_n^{(1)}$ firstly decreases and eventually vanishes with the rise of T. With the increase in value of J, the critical value of temperature T_c (T_c is defined as $T \geq T_c$, $E_n = 0$) firstly increases and then decreases. When $J = 1.2\kappa$ (the red dotted line), T_c reaches the maximum value of 1.6 K. For comparison, $E_n^{(1)}$ is plotted as a function of T with different values of nonreciprocal coupling strength J_2, and we have assumed that $J_1 = 1.2\kappa$. We find that $E_n^{(1)}$ also gradually decreases to zero with the increase in value of T. However, the critical value of temperature T_c continuously increases with J_2. When $J_2 = 3.6\kappa$ (the purple dotted-dashed line), T_c can reach 45 K, which is several orders of magnitude larger than the ground state temperature of the mechanical oscillator and is higher than that in Refs. [50,51]. Furthermore, T_c can rise further if J_2 increases further.

The logarithmic negativity $E_n^{(2)}$ is plotted as a function of the environment temperature T with different values of reciprocal coupling strength J in Fig. 4(c). We find a similar result that, T_c firstly increases and then decreases with the increase in value of J. When $J = 2\kappa$ (the red dashed line), T_c reaches the maximum value of 22 K. Furthermore, $E_n^{(2)}$ is plotted as a function of T with different values of nonreciprocal coupling strength J_1, and $J_2 = 2\kappa$ in Fig. 4(d). It is also found that $E_n^{(2)}$ gradually decreases to zero with the increase in T, and T_c continuously increases with J_1. When $J_1 = 2.6\kappa$ (the purple dotted-dashed line), T_c can reach 78 K.

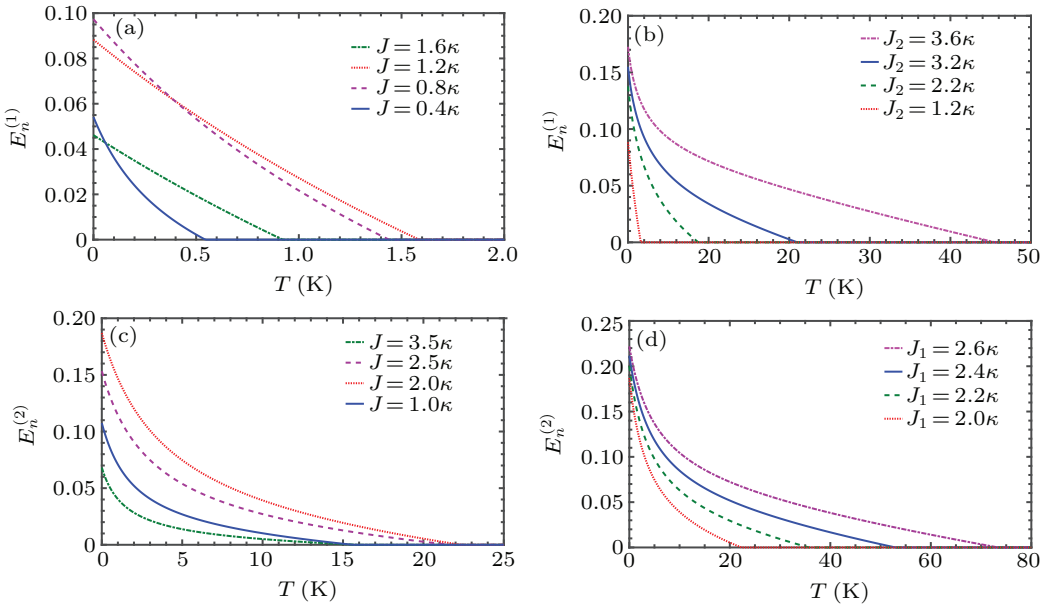


Fig. 4. (a), (c) The logarithmic negativity $E_n^{(1)}$ and $E_n^{(2)}$ as a function of the environment temperature T with different values of reciprocal coupling strength J. (b), (d) $E_n^{(1)}$ and $E_n^{(2)}$ as a function of T with different values of nonreciprocal coupling strength J_2 and J_1. (b) $J_1 = 1.2\kappa$, (d) $J_2 = 2\kappa$, and the other parameters can be found in the text.

4. Conclusion

In summary, we have studied the quantum entanglement in a double-cavity optomechanical system, which consists of an optomechanical cavity and an auxiliary cavity. The optomechanical cavity mode couples with the mechanical mode via radiation-pressure interaction, and simultaneously couples with the auxiliary cavity mode via nonreciprocal coupling. We adopt the logarithmic negativity $E_n^{(1)}$ ($E_n^{(2)}$) to quantify the entanglement degree between the mechanical mode and the optomechanical cavity mode (the auxiliary cavity mode). We show $E_n^{(1)}$ and $E_n^{(2)}$ in the case of reciprocal coupling, and find that both $E_n^{(1)}$ and $E_n^{(2)}$ have maximum values. However, $E_n^{(1)}$ and $E_n^{(2)}$ can exceed those maximum values by using nonreciprocal coupling, and a wider detuning region where the entanglement exists can be obtained. Moreover, we also demonstrated the influence of environment temperature on $E_n^{(1)}$ and $E_n^{(2)}$, and the results indicate that the nonreciprocal coupling can effectively enhance the entanglement robustness. The proposed scheme provides an easier way to experimentally realize and observe the optomechanical entanglement.

Acknowledgement

Project supported by the National Natural Science Foundation of China (Grant Nos. 12047520, 61941501, 61775062, 11574092, 61378012, 91121023, 62071186 and 61771205).

References

[1] Aspelmeyer M, Kippenberg T J and Marquardt F 2013 *Rev. Mod. Phys.* **86** 1391
[2] Kippenberg T J and Vahala K J 2008 *Science* **321** 1172
[3] Buonanno A and Chen Y 2002 *Phys. Rev. D* **65** 042001
[4] Ji R Q, Yang L, Zhang L, Tian Y H, Ding J F, Chen H T, Lu Y Y, Zhou P and Zhu W W 2011 *Opt. Express* **19** 20258
[5] Giovannetti V, Lloyd S and Maccone L 2011 *Nat. Photonics* **5** 222
[6] Bai C H, Wang D Y, Wang H F, Zhu A D and Zhang S 2016 *Sic. Rep.* **6** 33404
[7] Ho M, Oudot E, Bancal J D and Sangouard N 2018 *Phys. Rev. Lett.* **121** 023602
[8] Zhang Z C and Wang X G 2020 *Opt. Express* **28** 2732
[9] Shen R C, Zhang G Q, Wang Y P and You J Q 2019 *Acta Phys. Sin.* **68** 230305 (in Chinese)
[10] Fabre C, Pinard M, Bourzeix S, Heidmann A, Giacobino E and Reynaud S 1994 *Phys. Rev. A* **49** 1337
[11] Brooks D W C, Botter T, Schreppler S, Purdy T P, Brahms N and Stamper-Kurn D M 2012 *Nature* **488** 476
[12] Lü X Y, Wu Y, Johansson J R, Jing H, Zhang J and Nori F 2015 *Phys. Rev. Lett.* **114** 93602
[13] Zhang Z C, Wang Y P, Yu Y F and Zhang Z M 2018 *Opt. Express* **26** 11915.
[14] Rabl P 2011 *Phys. Rev. Lett.* **107** 063601
[15] Lemonde M A, Didier N and Clerk A A 2014 *Phys. Rev. A* **90** 063824
[16] Huang R, Miranowicz A, Liao J Q, Nori F and Jing H 2018 *Phys. Rev. Lett.* **121** 153601
[17] Wang K, Wu Q, Yu Y F and Zhang Z M 2019 *Phys. Rev. A* **100** 053832
[18] Liu J, Yang J Y, Liu H and Zhu A D 2020 *Opt. Express* **28** 18397
[19] Xiao Y M, Liu J H, Wu Q, Yu Y F and Zhang Z M 2020 *Chin. Phys. B* **29** 074204
[20] Horodecki R, Horodecki P, Horodecki M and Horodecki K 2009 *Rev. Mod. Phys.* **81** 865
[21] DiVincenzo D P 1995 *Science* **270** 255
[22] Fabre C, Pinard M, Bourzeix S, Heidmann A, Giacobino E and Reynaud S 1994 *Phys. Rev. A* **49** 1337
[23] Bennett C H and DiVincenz D P 2000 *Nature* **404** 247
[24] Vitali D, Gigan S, Ferreira A, Böhm H R, Tombesi P, Guerreiro A, Vedral V, Zeilinger A and Aspelmeyer M 2007 *Phys. Rev. Lett.* **98** 030405
[25] Akram U, Munro W, Nemoto K and Milburn G J 2012 *Phys. Rev. A* **86** 042306
[26] Liao J Q, Wu Q Q and Nori F 2014 *Phys. Rev. A* **89** 014302
[27] Liu J H, Zhang Y B, Yu Y F and Zhang Z M 2017 *Opt. Express* **25** 7592
[28] Xu X W, Shi H Q, Liao J Q and Chen A X 2019 *Phys. Rev. A* **100** 053802
[29] Jiao Y F, Zhang S D, Zhang Y L, Miranowicz A, Kuang L M and Jing H 2020 *Phys. Rev. Lett.* **125** 143605
[30] Bender and Carl M 2007 *Rep. Prog. Phys.* **70** 947
[31] Miri M A and Alù A 2019 *Science* **363** eaar7709
[32] He L, Özdemir S K, Xiao Y and Yang L 2010 *IEEE J. Quantum Electron.* **46** 1626
[33] Bender C M and Boettcher S 1998 *Phys. Rev. Lett.* **80** 5243
[34] Yao S and Wang Z 2018 *Phys. Rev. Lett.* **121** 13680
[35] Lieu S 2018 *Phys. Rev. B* **97** 045106
[36] Yin C, Jiang H, Li L, Lü R and Chen S 2018 *Phys. Rev. A* **97** 052115
[37] Wang D Y, Bai C H, Liu S, Zhang S and Wang H F 2020 *New J. Phys.* **22** 093006
[38] Hatano N and Nelson D R 1996 *Phys. Rev. Lett.* **77** 570
[39] Longhi S, Gatti D, and Della Valle G 2015 *Phys. Rev. B* **92** 094204
[40] Shen Y, Bradford M and Shen J T 2011 *Phys. Rev. Lett.* **107** 173902
[41] Longhi S, Gatti D and Della Valle G 2015 *Sci. Rep.* **5** 13376
[42] Zhu X, Wang H, Gupta S K, Zhang H, Xie B, Lu M and Chen Y 2020 *Phys. Rev. Res.* **2** 013280
[43] Gardiner C W and Zoller P 2000 *Quantum Noise* (Berlin: Springer)
[44] DeJesus E X and Kaufman C 1987 *Phys. Rev. A* **35** 5288
[45] Adesso G, Serafini A and Illuminati F 2004 *Phys. Rev. A* **70** 022318
[46] Kleckner D, Marshall W, Dood M J A D, Dinyari K N , Pors B J, Irvine W and Bouwmeester D 2006 *Phys. Rev. Lett.* **96** 173901
[47] Gigan S, Böhm H R, Paternostro M, Blaser F, Langer G, Hertzberg J B, Schwab K C, Bäuerle D, Aspelmeyer M and Zeilinger A 2006 *Nature* **444** 67
[48] Arcizet O, Cohadon P F, Briant T, Pinard M and Heidmann A 2006 *Nature* **444** 71
[49] Yousif T, Zhou W and Zhou L 2014 *J. Mod. Opt.* **61** 1180
[50] Vitali D, Gigan S, Ferreira A, Böhm H R, Tombesi P, Guerreiro A, Vedral V, Zeilinger A and Aspelmeyer M 2007 *Phys. Rev. Lett.* **98** 030405
[51] Genes C, Vitali D and Tombesi P 2008 *Phys. Rev. A* **77** 050307